Photoacoustic Depth Profiling of Polymer Laminates by Step-Scan Fourier Transform Infrared Spectroscopy

REBECCA M. DITTMAR, JAMES L. CHAO, and RICHARD A. PALMER*

Department of Chemistry, Duke University, Durham, North Carolina 27706 (R.M.D., R.A.P.); and IBM Corporation, Research Triangle Park, North Carolina 27709 (J.L.C.)

The use of step-scan Fourier transform infrared (FT-IR) spectroscopy with photoacoustic (PA) detection for depth profiling studies of polymer laminates is demonstrated. Step-scan FT-IR simplifies the extraction of depth profile information due to the single modulation frequency that can be applied over the entire spectral range. Because a single modulation frequency is generally used in step-scan FT-IR, the thermal diffusion length, μ, is constant for all wavelengths in a single scan. In addition, lock-in detection allows for easy extraction of the signal phase. Two methods of depth profiling are discussed and illustrated. The first is the conventional method of varying the probe depth by changing the modulation frequency. The other method depends on the direct use of the signal phase. The phase analysis technique is particularly useful for cleanly separating the signal due to a thin (<5 μm) surface layer from that of the bulk or substrate.

Index Headings: Depth profiling; FT-IR/PAS; PAS; Infrared; Polymer films; Polymer spectroscopy; Step-scan FT-IR.

INTRODUCTION

Fourier transform infrared (FT-IR) spectroscopy combined with photoacoustic (PA) detection is used for the analysis of a large variety of materials.[1-8] While most commercial FT-IR spectrometers operate with rapid-scan interferometers, there is a growing interest in step-scan interferometers due to their intrinsically more facile application to dynamic spectroscopy, including condensed-phase photoacoustic spectroscopy (PAS).[9-15] Although PAS is not generally classified as time-resolved or dynamic spectroscopy, the relatively slow process of thermal diffusion creates a phase lag in the PA response analogous to that of other dynamic processes. The main advantage of step-scan interferometry for PAS (particularly in the frequency domain) is that a single (constant) modulation frequency can be applied over the entire spectral range to generate the PA signal. (In contrast, although the intrinsic Fourier modulation of the IR beam in rapid-scan FT-IR can be conveniently used to generate a PA signal, each wavelength, λ, is modulated at its own frequency, $F = 2v/\lambda$, where v is the mirror velocity.) In the step-scan mode, the single modulation frequency allows a lock-in amplifier to be used to detect and amplify the PA signal at each point in the interferogram. This use of a phase-sensitive detector facilitates the extraction of phase information, which, along with variation of the modulation frequency, is very useful in PA depth profiling experiments.

The focus of this paper is on the ability of PAS to depth profile layered materials.[1,2,5-8,16-23] Both the PA signal strength and the thermal diffusion length, μ, are inversely dependent on the modulation frequency. The thermal diffusion length[34] is defined as $\mu = (\kappa/\rho C_p \pi f)^{1/2}$ where κ is the thermal conductivity, ρ is the density, C_p is the heat capacity, and f is the modulation frequency (Hz). The way in which μ is related to the photothermal probe depth can be understood as described below.

For an optically and thermally homogeneous sample the photothermal source term is proportional to $\beta e^{-\beta(\lambda)x}$, where $\beta(\lambda)$ is the absorptivity at wavelength λ, and x is the distance into the sample. Thus, the radiation is damped (extinguished) and the deposited heat is reduced by a factor of $1/e$, $1/e^2$, and $1/e^{2\pi}$ at penetration depths of $x = \ell_\beta$, $2\ell_\beta$, and $2\pi\ell_\beta$, respectively, where $\ell_\beta = 1/\beta$. Likewise, the thermal wave reaching the surface is damped by a factor of e^{-ax}, where the thermal diffusion coefficient $a = 1/\mu$. Thus, for heat deposited at $x = \mu$, 2μ, and $2\pi\mu$ beneath the surface, the thermal wave will be damped by $1/e$, $1/e^2$, and $1/e^{2\pi}$, respectively.[23] The combined effect of the "optical damping" and thermal damping works to ensure that essentially only heat deposited within a distance μ of the surface gives rise to a detectable modulation of the surface temperature in a homogeneous sample.

However, for an optically inhomogeneous sample the situation may be quite different.[24] Consider the case of a laminar sample which, for some range of wavelengths λ, consists of one or more *transparent* surface layers and a strongly absorbing under layer. For the wavelength range of surface layer transparency ($\beta = 0$), the radiation arrives undiminished at the absorbing layer; there it is extinguished within a layer of thickness $\ll\mu$ (for the absorbing layer). In the limit of an infinitely thin absorbing layer, the resulting thermal wave is then damped by e^{-ax} before reaching the surface, where x is now the combined thickness of the transparent surface layers, and $a = 1/\mu$ for the surface layer(s). (If the layer in which the heat is deposited is of finite thickness, further thermal wave damping will occur.) Thus, in principle, a signal-to-noise ratio of greater than 20 ($\sim e^3$) would permit detection of a strongly absorbing subsurface layer from beneath a transparent surface layer as thick as three times the thermal diffusion depth of the surface layer. With a signal-to-noise ratio of 10^3, a strongly absorbing layer as deep as $2\pi\mu$ beneath a transparent superficial layer might be detected. However, any absorption in the surface layer would rapidly reduce the maximum probe depth toward μ again, effectively masking the under layer for those wavelengths absorbed.

In either the case of the homogeneous sample or that of the transparent surface layer sample, the effect of a 10-fold change in modulation frequency f would be a change by a factor of ~3 in effective maximum probe depth. (This observation presumes that the homoge-

Received 2 January 1991; revision received 18 April 1981.
* Author to whom correspondence should be sent.

0003-7028/91/4507-1104$2.00/0

TABLE I. Thermal properties and thermal diffusion depths.

	κ (W/mK)	ρ (g/cm³)	C_p (J/gK)	μ (μm) (100 Hz)	(μm) (200 Hz)	(μm) (800 Hz)
Elvax®	0.253–0.332	0.948	2.30[a]	20.5	14.5	7.3
Polypropylene	0.135[b]	0.902[c]	1.926[c]	15.7	11.1	5.6
Kapton®[d]	0.15	1.42	1.09	18	12	6.2
Teflon®[d]	0.207	2.15	1.172	16.2	11.4	5.7

[a] See Ref. 25.
[b] See Ref. 26.
[c] See Ref. 27.
[d] See Ref. 28.

neous sample is not photothermally saturated and that the subsurface layer of the heterogeneous sample is strongly absorbing.) For the homogeneous sample, increasing the modulation frequency is a method of reducing or eliminating saturation. However, for the heterogeneous sample, successive increases in f restrict detection to layers closer and closer to the surface.

For the heterogeneous sample, difference spectra of scans collected in a sequence of modulation frequencies can be used to isolate spectra of absorbing species at different depths. For example, for the polymers studied here, $2\pi\ \mu$ ($\sim 6\ \mu$) is about 70 μm at 200 Hz and 50 μm at 400 Hz (Table I). Thus, in principle, a subsurface layer at a depth of 60 μm might be identified in the difference between the 200-Hz and 400-Hz spectra, provided that this layer absorbed strongly in a region of transparency of the surface layer(s). The practical signal-to-noise ratio in these FT-IR experiments actually makes the limiting detection depth closer to 2–3 μ rather than 6 μ; that is, a discrimination between roughly 20 and 30 μm for 400 and 200 Hz is feasible. Step-scan data collection for such depth profiling experiments produces a constant sampling depth across the spectrum for each frequency used.

The phase of the signal can also be used for PA depth profiling. This possibility has been recognized since the early days of the photoacoustic revival, but has been exploited only to a limited extent.[1,20–22,29] Analysis of the PA phase has the ability to provide more precise information about the depth of the absorbing species than does the variation of modulation frequency alone.[1] However, use of the phase in FT-IR/PAS has, in the past, been complicated by the addition of the beamsplitter phase and the PA phase in rapid-scan FT-IR. This addition is eliminated in step-scan FT-IR.

The use of the phase for depth profiling is based on the theoretical prediction, in the absence of slow deexcitation processes, that the time it takes for the heat to transfer from a given point in the sample to the illuminated surface is the rate-determining step for PA signal detection. Adams and Kirkbright and co-workers[20,21] were the first to use this principle, applying it to the analysis of biological samples in the visible region of the electromagnetic spectrum, and were able to distinguish between surface and bulk components.

More recently, depth profiling by phase analysis has been demonstrated in the mid-IR. Mongeau *et al.* have described a method for the separation of surface and bulk absorption in photothermal spectroscopy using photothermal beam deflection (PBDS, or the mirage effect).[22] Although the experimental setup for a PBDS experiment is different from that for PAS, the same general theory of thermal diffusion applies to both techniques.

According to Rosencwaig and Gersho (the R-G theory),[23] the PA signal originating from a strongly absorbing (completely photothermally saturated), thermally thick ($\ell > \mu$), homogeneous sample should be in-quadrature with the modulation. As pointed out by Mongeau *et al.*,[22] it follows that the phase of the signal from a thermally thin film ($\ell < \mu$) on the surface of a thermally thick substrate should also be in-quadrature. In addition, for a homogeneous, thermally thick sample, the signal from a weak absorber should differ from that from a strong absorber by exactly 45°. Therefore, in the case of a two-layer sample, this observation leads directly to a strategy for separate detection of the absorption of a thin surface film and its substrate (provided that both are weakly absorbing).[22]

The phase relationships for the surface, bulk, and total signal in a two-layered sample consisting of a thermally thin, weakly absorbing surface layer on a thermally thick, weakly absorbing substrate are illustrated in Fig. 1. Because the surface and bulk signals are separated by only 45°, they cannot be isolated simultaneously by use of a two-phase lock-in amplifier. As shown in Fig. 1, the response at 90° contains both the surface signal and a component of the bulk signal. Likewise, the response at 135° contains a contribution from the surface. However, by setting the lock-in amplifier phase orthogonal to one or

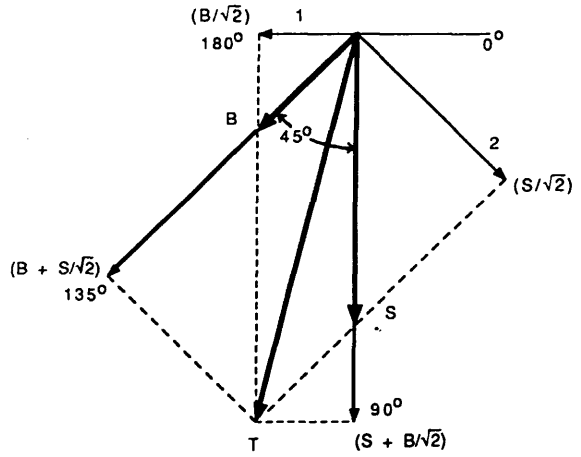

FIG. 1. Photoacoustic phase relationships for a thermally thin layer on a weakly absorbing substrate. Actual signals are indicated by ➡; signals detected at specific phase angles are indicated by ➡.

the other of the surface or bulk signals, one eliminates that component from the response. The signal detected is then either $S/\sqrt{2}$ or $B/\sqrt{2}$, as indicated in Fig. 1.

The detected PA phase, ϕ_T, includes both the PA phase of the sample (Fig. 1), as well as an instrumental phase, ϕ_0, which is determined by the geometric, optical, and electronic characteristics of the experiment. For example, the surface signal should be in-quadrature, as illustrated in Fig. 1; however, the actual surface signal will be shifted by an amount dependent on the value of ϕ_0. Although prior knowledge of the spectra of the surface and bulk components permits easy separation of their signals by rotation of the phase of the data after collection is complete, *a priori* identification of the surface vs. bulk components is greatly aided by establishment of a phase reference. One way to do this is to use a completely saturated strong absorber as a reference sample, since it will have all of its absorption localized near the surface.

The lock-in detector phase setting required to maximize the signal from this saturated absorber in one channel of a two-phase lock-in amplifier will be the same as that required to maximize the signal from a thermally thin absorber at the surface. (Practically, this equivalence also depends on the sample and reference having the same volume and shape, so as to produce identical ϕ_0's). When the reference is replaced by the sample, the bulk signal (vector 1, Fig. 1) multiplied by cos 45° should be in the channel orthogonal to the reference phase. The surface signal, free of contribution from the bulk, may be detected by advancing the phase by 45° (if the substrate is weakly absorbing), to give a signal equal to the surface signal multiplied by cos 45° (vector 2, Fig. 1). (It should be noted that the instrumental phase is a function of the modulation frequency, and therefore, the reference and sample phases must be determined at the same frequency).

When one is using a single-phase lock-in amplifier, the phase settings are made as described above, although more than one scan will be needed to extract all of the information. Another possibility is to use two separate single-phase lock-in detectors with their phases set 135° apart (at the proper offsets relative to the reference phase) so as to detect $S/\sqrt{2}$ and $B/\sqrt{2}$ directly, as shown in Fig. 1. However, as mentioned above, when one is using a two-phase lock-in amplifier, it is convenient to set one channel to isolate the bulk signal. After the "in-phase" and "quadrature" interferograms have been collected, they can be manipulated by rotation of their relative phases in order to correct for any ϕ_0 difference between the sample and reference and also to isolate the surface signal. In fact, with a two-phase lock-in detector, the initial phase offset can be arbitrary if the spectrum of the surface film or the substrate is known, since the phase can always be rotated after data collection is complete to maximize the separation of the surface signal and that of the bulk. With either the two-phase lock-in amplifier or two single-phase lock-in amplifiers, both signals are determined simultaneously in a single (step) scan.

The technique outlined above is a method of depth-profiling which, strictly speaking, works only for thermally thin, weakly absorbing films on thermally thick, weakly absorbing substrates.[22] In practice, however, it can be extended qualitatively to samples which do not exactly meet these strict criteria. For example, the absorptivity of the surface film can be high, and its phase will still be distinctive, provided that the absorption of the bulk at the same wavelength is weak. However, strong absorption by the surface will effectively prevent radiation penetration and will mask the signal from the bulk at those wavelengths. On the other hand, strong absorption by the substrate will reduce the phase separation between surface and substrate signals. Likewise, as the surface film becomes thermally thick, it will begin to thermally mask the bulk signal, causing the phase lag of the bulk (substrate) relative to the true surface signal phase to be greater than the predicted 45°. The actual separation between the phases of the signals from the surface and bulk layers in this case will depend on the intensity of the surface and bulk absorptions and may approach 90° for surface layers which are strongly absorbing at some wavelengths but transparent at others, and are nearly thermally thick.

When such deviations from ideal conditions occur, empirical adjustment of the detection phase may be necessary, and different phase separations may be required for different regions of the spectrum. However, the use of the PA signal detection phase still often provides an easy and direct means to separate the absorption of a surface film from that of its substrate. In contrast, although phase analysis is possible in the rapid-scan mode, it must be done with the phase correction function inactivated; in addition, the wavelength dependence of the beamsplitter phase and the PA cell phase must be carefully compensated for by subtracting a reference phase spectrum, since each point in the phase spectrum corresponds to a different Fourier frequency.

EXPERIMENTAL

The spectra illustrated here were collected on a modified Nicolet IR42 FT-IR spectrometer (originally an IBM Instruments IR40) that is capable of collecting data in both the step-scan and the rapid-scan modes. This instrument is essentially identical to the step-scan IBM IR44 previously described.[9,15] However, phase-sensitive detectors (Evans Electronics, Inc., Berkeley, CA; Model 4110 PSD) have replaced the lock-in amplifiers in the control circuit, and the pulse generator has been replaced by a computer program that is capable of stepping the mirror rapidly for initial positioning. Also, a PARC Model 5210 two-phase lock-in amplifier is used to demodulate the "in-phase" and "quadrature" signals. The intensity modulation of the IR beam is produced by path difference (phase) modulation.

An MTEC Model 100 photoacoustic cell with its accompanying preamplifier/power supply was used to obtain all spectra. Helium was used as the carrier gas in the PA cell because of its superior thermal coupling properties. The spectrometer was purged with N_2 gas to remove atmospheric H_2O and CO_2. The interferograms were obtained by collecting data at approximately 2200 points separated by intervals of one wavelength of the reference HeNe laser, to obtain single-sided interferograms of 2048 points, plus 128 phase correction points, to give 8 cm^{-1} resolution. The in-phase (I) and quadrature (Q) interferograms were collected simultaneously and Fourier

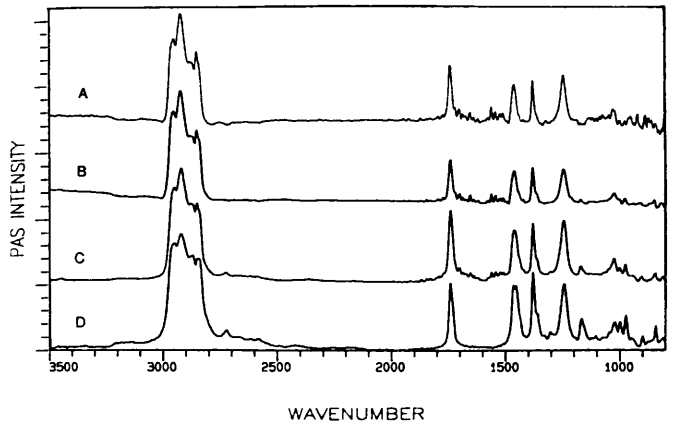

FIG. 2. Step-scan FT-IR/PA magnitude spectra of ethylene-vinyl acetate copolymer on polypropylene: (*A*) 800 Hz and $\frac{1}{2}\lambda_{HeNe}$; (*B*) 600 Hz and $1\lambda_{HeNe}$; (*C*) 400 Hz and $2\lambda_{HeNe}$; (*D*) 100 Hz and $2\lambda_{HeNe}$.

transformed after data collection was complete. From the in-phase and quadrature spectra, the magnitude [$M = (I^2 + Q^2)^{1/2}$] and phase [$\phi = \tan^{-1}(Q/I)$] spectra were calculated, if desired, or the individual components (I and Q) were used, as described above.

The ease and repeatability of filling the PA sample holder, as well as the sample uniformity, are important factors for obtaining reference spectra that will not add artifacts to the sample spectra.[3,4] For this reason carbon black powder, which is typically used to ratio all PA spectra to correct for the instrument response function, was not used in these studies. Instead, a condensed-phase, nonparticulate sample (60% carbon black-filled elastomer) was used to ratio all of the spectra. Because of the high percentage of carbon black, this sample provided the necessary correction for the instrument response function. In addition, it is nonporous and can be sized so as to have virtually the same cell filling factor as the sample and spacer; thus it was also a useful sample for determining the reference phase (see below). Each spectrum was ratioed against a reference spectrum collected at the same phase modulation frequency and amplitude.

Because the phase of the PA cell is dependent on a number of conditions, including the modulation frequency and the sample size, a cell spacer was designed to fill all but the top 1 mm of the sample space. This spacer was made of a thin slice of the 60% carbon black-filled elastomer underneath a 4-mm-thick KBr disk. The sample was placed on top of this KBr disk. The spacer also served as a trap for any thermal signal which could be generated by light transmitted by the sample.

Tests were run on the instrument and cell to determine the repeatability of the phase spectrum of the 60% carbon black-filled elastomer. For the same sample removed and reloaded into the cell, it was found that the phase varied by less than 1° from trial to trial. However, as mentioned above, in many cases the exact setting of the reference phase is not necessary since maximum distinction of the surface and bulk signals is easily obtainable by applying the phase rotation operation to the I and Q interferograms after data collection.

Two different polymer samples are used to illustrate depth profiling in this paper. The first is a DuPont Elvax® vinyl resin (grade 360) cast from a benzene solution onto a 60-μm-thick polypropylene substrate. The Elvax® vinyl resin is an ethylene-vinyl acetate (EVA) copolymer received in pellet form. The second sample is a DuPont Kapton® polyimide film (200FN919) which is 50 μm thick and comprised of polyimide sandwiched between two 12.5-μm-thick layers of Teflon® FEP. The thermal properties for each of these samples are found in Table I, along with calculated thermal diffusion depths.

For the phase analysis studies, the reference sample was placed in the PA cell to determine the correct phase of the lock-in amplifier at each phase modulation (PM) frequency to be used. The correct phase was determined first by stepping the mirror to the zero retardation point, which is the point in the interferogram that contains contributions from all wavelengths. Then the lock-in amplifier phase was rotated until all the signal was located in the quadrature channel. Once the correct lock-in amplifier phase was found, the reference was replaced by the sample, and the signal was simultaneously collected at that phase (Q) and orthogonal to it (I).

Transformation of the I and Q interferograms collected as described above generally reveals significant separation of the surface and bulk spectra. However, additional distinction can usually be achieved by computer rotation of the phases of the two vector components.[30] The computer program is based on simple vector mathematics illustrated by $[e^{i\vartheta}(me^{i\phi}) = me^{i(\vartheta+\phi)} = m\cos^{(\vartheta+\phi)} + im\sin^{(\vartheta+\phi)}]$, where $e^{i\vartheta}$ is the polar representation of the phase rotation angle ϑ, and $me^{i\phi}$ is the polar representation of a pair of points in the original interferograms (I and Q).

RESULTS

Figure 2 illustrates PA depth profiling obtained by varying the modulation frequency, and, thus, varying the thermal diffusion depth. The four magnitude spectra in Fig. 2 are of the ethylene-vinyl acetate (EVA) copolymer on a polypropylene (PP) substrate, collected at phase modulation (PM) frequencies and amplitudes of: (*A*) 800 Hz and $\frac{1}{2}\lambda_{HeNe}$; (*B*) 600 Hz and $1\lambda_{HeNe}$; (*C*) 400 Hz and $2\lambda_{HeNe}$; and (*D*) 100 Hz and $2\lambda_{HeNe}$. In this sample the EVA layer is approximately 12 μm thick and the PP is about 60 μm thick.

Depth profiling by use of phase analysis, on the same sample, is shown in Fig. 3. Spectra *B* and *D* of Fig. 3 show two vector components of the spectrum of the EVA copolymer on PP separated by a detection phase of 135°, obtained from data measured in a single scan at a PM frequency of 100 Hz. (Calculating the square root of the sum of the squares of these two vector components gives the 100 Hz magnitude spectrum shown in Fig. 2D.)

Another example of the phase analysis for separation of surface and bulk signals is shown in Fig. 4, which contains the magnitude (*A*), in-phase (*C*), and quadrature (*E*) spectra of Kapton® polyimide, as well as the separately determined spectra of Teflon® (*D*) and the polyimide (*B*), all collected at a PM frequency of 200 Hz.

DISCUSSION

Depth profiling based simply on changing the modulation frequency provides valuable information, even though the results are not as dramatic as for those ob-

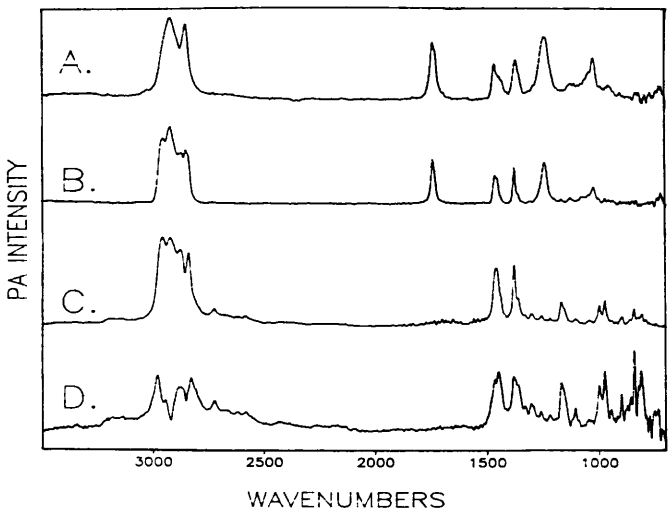

FIG. 3. Step-scan FT-IR/PA phase-separated spectra of 12-μm-thick ethylene-vinyl acetate copolymer (EVA) on 60 μm-thick polypropylene (PP) (*B* and *D*, respectively) compared to separately determined PA spectra of individual components (*A* and *C*). The phase angle difference between vector components *B* and *D* is 135°. All measurements were made with a phase modulation frequency of 100 Hz and amplitude of $2\lambda_{HeNe}$. The vector component *D* (bulk) has been multiplied by a factor of 3.0 relative to spectrum *B* (surface).

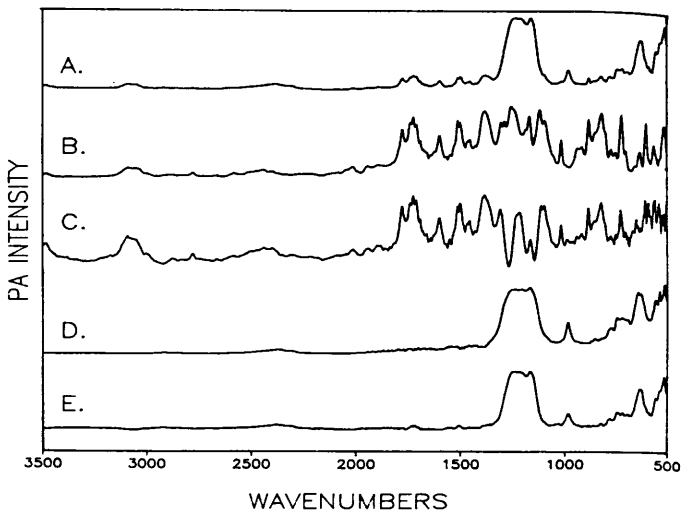

FIG. 4. Step-scan FT-IR/PA phase-separated spectra of Kapton® polyimide film—(*C*) in-phase, ~ bulk, polyimide; (*E*) quadrature, ~ surface, Teflon®; and (*A*) conventional magnitude $q = (I^2 = Q^2)^{1/2}$—compared to separately determined PA spectra of the individual components (*B* and *D*). All measurements were made at a phase modulation frequency of 200 Hz and amplitude of $2\lambda_{HeNe}$. The vector component *C* (bulk) has been multiplied by a factor of 4.8 relative to spectrum *E* (surface).

tained by use of the phase. The spectra in Fig. 2 can be analyzed by comparing the relative intensities of bands that are from the two different layers and seeing how these intensities change at different modulation frequencies. As expected, the 800-Hz signal consists almost entirely of the spectrum of the EVA, since at this frequency its thermal diffusion depth $\mu = 7.3$ μm. In the progression toward lower modulation frequencies, the thermal diffusion length increases, and, again, as expected, the spectra include an increasing proportion of the bulk (PP) signal. Thus, in the 100-Hz spectrum there are major contributions from both the surface and bulk layers, since at this frequency the EVA layer is thermally thin ($\mu = 20.5$ μm). To obtain depth profiling information from these spectra, one can compare the relative integrated intensities of bands that are known to be from the two different layers. In the absence of prior knowledge of the spectra of the surface and/or bulk layers, the pattern of band intensity changes can be used as a qualitative identifier of surface and bulk components. In some cases, subtraction of spectra obtained at different modulation frequencies yields useful depth profiling information. However, subtraction cannot be used in regions of saturation due to the non-uniformity of peak shapes. It is also necessary to take into account the frequency dependence of the PA signal intensity for a valid subtraction.

In the EVA-on-PP sample of Fig. 2, the relative integrated intensities of the carbonyl stretch at 1730 cm^{-1} (from the surface layer), the C-H bends at 1370 and 1450 cm^{-1} (from the surface and bulk layers), the C-C lattice vibration at 1160 cm^{-1} (from the bulk layer), and the C-H stretching peaks at 2918 and 2850 cm^{-1} can be analyzed to determine the different layers from which the bands originate. In the 800-Hz spectrum the carbonyl stretch is the largest peak, much larger than the two C-H bending peaks at 1370 and 1450 cm^{-1}, and the C-C peak at 1160 cm^{-1} cannot be seen. Therefore, the EVA must be on the surface while the PP is the bulk. This conclusion is supported by the 100-Hz spectrum, where the intensities of the carbonyl band at 1730 cm^{-1} and the C-H bending peaks at 1370 and 1450 cm^{-1} are approximately equal, meaning that more of the PP layer is contributing to the spectrum due to the greater thermal diffusion length. Also, the C-C peak at 1160 cm^{-1} in the 100-Hz spectrum is a fairly intense peak due to the greater depth being sampled (surface and bulk) at this frequency. The intensity of the peak at 1160 cm^{-1} is a good demonstration of the progression of increasing thermal diffusion length with decreasing modulation frequency, since the peak is non-existent at 800 Hz and has increased to medium intensity in the 100-Hz spectrum. In conclusion, Fig. 2 does give some depth profiling information, but it does not provide a simple way to get a clean separation of the surface and bulk signals.

The same EVA-on-PP sample was used to illustrate depth profiling by phase analysis (Fig. 3). The 100-Hz magnitude spectrum of EVA on PP in Fig. 2 has been separated into two vector components 135° apart in Fig. 3 (spectra *B* and *D*). Spectrum *B* is a representation of the surface spectrum, EVA, and spectrum *D*, of the bulk spectrum, PP. For comparison purposes the separately determined spectra of EVA and PP are also shown (spectra *A* and *C*, respectively). Since the surface EVA layer in this sample is thermally thin, the separation of the two spectra is in agreement with the vector diagram in Fig. 1. Spectra *B* and *D* closely resemble the spectra of EVA and PP, respectively, but are not exact replicas.

The differences between the phase-separated surface and bulk spectra and the true spectra of EVA and PP can be understood in light of the previous discussions. For example, the phase of the bulk spectrum is dependent on the absorption coefficient at each wavelength; as a result, the vector component of the signal 90° away

from the surface signal may not contain a uniform proportion of the bulk signal at each wavelength. This is demonstrated by spectrum *D* in Fig. 3, where the absorptions that are relatively weak in a pure PP spectrum (all the bands below 1160 cm^{-1}) are relatively strong in comparison to the C-H bends at 1370 and 1450 cm^{-1}. This result occurs because the phase of the C-H bends is less than 45° from the surface phase. Also, the cutout in the C-H stretching region of spectrum *D* occurs because the surface layer absorbs most of the light in that region, eliminating true bulk absorption. However, the resemblance of spectrum *D* to that of a pure PP sample is close enough to permit a qualitative determination of the composition of the bulk layer. The comparison of the two EVA spectra (*A* and *B*) also shows a few subtle differences. For example, in the C-H stretch region in spectrum *B*, the two peaks at 2920 and 2850 cm^{-1} are the main absorptions, but shoulders and small peaks that correspond to PP absorption also occur. PP is highly absorbing in the C-H stretch region and, therefore, the phase of the C-H stretch absorptions approaches the phase of the surface absorptions.

Figure 4 illustrates the ability to obtain the spectrum of a subsurface layer, which in this case is polyimide. For this sample the best separation of surface and bulk signals is given by the initial *I* and *Q* spectra collected at a PM frequency of 200 Hz and amplitude of $2\lambda_{HeNe}$. Detecting the surface and bulk signals 90° apart is experimentally very simple, since this procedure corresponds to analyzing the in-phase and quadrature channels directly off the lock-in detector without need for additional computer phase rotation. In Fig. 4, the in-phase spectrum (*C*) is proportional to the signal from the bulk, which is polyimide for the depth obtainable at this modulation frequency. The quadrature spectrum (*E*) is proportional to the signal from the surface layer (12.5 μm Teflon® FEP). Although the distinction of the surface and bulk signals is complete with the 90° phase angle difference, the in-phase polyimide spectrum is extensively masked, and thus badly distorted, in the region of the very intense C-F stretching peak from the Teflon®. More complete separation of the surface and bulk signals by use of phase rotation was not possible in this case.

The 90° separation between the surface and bulk signal phases occurs mainly because of the thickness of the top Teflon® layer and the intensity of the C-F stretch. The surface Teflon® layer is 12.5 μm thick, whereas μ for Teflon® at 200 Hz is 11 μm. Thus, the surface layer is almost thermally thick. Because of this, the centroid of absorption (and thus of heat distribution) of the polyimide interior layer is significantly further from the surface than is assumed in Fig. 1. As a result, the phase of the polyimide (bulk) signal is shifted significantly clockwise (a phase lag approaching 90° relative to the surface reference phase). However, the major band of the surface (Teflon®) layer is so strong that, in that region of the spectrum, it is almost optically opaque. Thus, despite the thickness of the Teflon®, the phase of this band is not shifted significantly from the phase of the reference. Consequently, the initial phase settings based on the phase of the carbon-black-filled elastomer signal (*Q*) and the signal orthogonal to it give an almost clean distinction of the spectra of the top two layers of the sample.

SUMMARY

FT-IR/PA depth profiling can be achieved with relative ease and flexibility with the use of step-scan data collection, either by varying the modulation frequency or by making direct use of the signal phase. The use of a single modulation frequency for each scan gives a constant thermal diffusion length, μ, across the spectrum, which means a constant sampling depth (in the absence of photothermal saturation). The single modulation frequency also allows the use of lock-in detection and the simple extraction of the in-phase (*I*) and quadrature (*Q*) components of the PA response. From the transforms of the *I* and *Q* interferograms, the PA magnitude and relative phase spectra may be calculated. However, for the purpose of distinguishing the absorption of a surface layer from that of its substrate, the *I* and *Q* spectra may be used directly, or their phases may be rotated until the desired separation is achieved.

The phase method works most efficiently and simply when neither the surface layer nor the bulk (substrate) is strongly absorbing and when the surface layer is truly thermally thin. As long as the surface layer is thermally thin, the phase of its signal remains constant, regardless of its absorptivity. However, the phase of the bulk signal changes with its absorbance and may vary widely over the spectral range, thus producing significant differences in the phase angle necessary to provide a separation of the surface and bulk signals. Likewise, for surface layers which are near thermal thickness, the phase separation may differ significantly from that predicted for the ideal case. In such situations, empirical rotation of the signal phase to achieve maximum distinction of surface and bulk spectra is still relatively easy. However, strong absorption by the surface layer will mask the signal from the substrate at those wavelengths.

The depth and depth resolution that are attainable by this phase analysis technique are dependent on a number of conditions. The depth being probed is determined by the optical properties of the sample and also by the thermal diffusion length, which itself is dependent on the thermal characteristics of the sample, as well as being inversely dependent on the modulation frequency. Within the limits imposed by the wavelength-dependent optical penetration depth and the limitations of the instrumentation, experimental variation of the modulation frequency can be used to control the total depth probed. For the instrument described here, a phase modulation frequency of about 100 Hz is the lowest that is currently available. This corresponds to a ~16 μm thermal diffusion length for a typical polymer, so that the maximum theoretical probe depth beneath a transparent surface layer ($2\pi\mu$) is on the order of 100 ± 10 μm (although in most practical situations signals from beneath a layer of >3 μ are difficult to detect). Thin surface layers can be probed more efficiently by collecting spectra at high modulation frequencies. For the instrument described here, a modulation frequency of 1 kHz is a practical maximum. For samples such as those illustrated here, this translates to a probe depth of ~30 μm (practically, ~15 μm).

Once the maximum probe depth has been determined by choice of the modulation frequency, analysis of the phase of the response can then be used to discriminate

among the spectra of layers within in this depth. For samples such as those illustrated here, with a modulation frequency of 400 Hz and thus a μ of ~ 9 μm, and under the assumption of an accuracy of phase determination of $\pm 1°$, a depth resolution of ~ 24 μm/30 = 0.8 μm should be possible in a depth range of ~ 3–27 μm. This projection is based on the approximation from the R-G theory that the phase changes by $\sim 30°$ and has a slope of ~ 1 between the limits $\sim \mu/3$ and ~ 3 μ. Higher depth resolution and resolution closer to the surface should be possible at higher modulation frequencies. However, limitations imposed by weak absorptivity (which become more important at higher frequencies), as well as sample heating effects (which may be significant if the source intensity is increased), must be considered in efforts to increase resolution. More general application of this technique to multi-layered samples is the subject of ongoing work.

ACKNOWLEDGMENTS

The authors wish to thank Chris Manning for helpful discussions, and Susan Plunkett for assistance in data collection. Partial support of this work was provided by IBM Corporation and Duke University. The support and the provision of samples by R. O. Carter of Ford Motor Company Research Laboratories are also gratefully acknowledged.

1. L. Bertrand, Appl. Spectrosc. **42,** 134 (1988).
2. J. A. Gardella, Jr., G. L. Grobe III, W. L. Hopson, and E. M. Eyring, Anal. Chem. **56,** 1169 (1984).
3. R. O. Carter III and M. C. Paputa Peck, Appl. Spectrosc. **43,** 468 (1989).
4. R. O. Carter III, M. C. Paputa Peck, M. A. Samus, and P. C. Killgoar, Jr., Appl. Spectrosc. **43,** 1350 (1989).
5. T. Zerlia, Appl. Spectrosc. **40,** 214 (1986).
6. J. Philippaerts, E. Vanderheyden, and E. F. Vansant, Mikrochim. Acta [Wien] **II,** 145 (1988).
7. M. W. Urban and J. L. Koenig, Applied Spectrosc. **40,** 994 (1986).
8. C. Q. Yang, R. R. Bresee, and W. G. Fateley, Appl. Spectrosc. **41,** 889 (1987).
9. M. J. Smith, C. J. Manning, R. A. Palmer, and J. L. Chao, Appl. Spectrosc. **42,** 546 (1988).
10. K. H. Michaelian, Infrared Phys. **30,** 181 (1990).
11. K. H. Michaelian, Appl. Spectrosc. **43,** 185 (1989).
12. K. H. Michaelian, Infrared Phys. **29,** 87 (1989).
13. B. Lerner, J. H. Perkins, G. L. Pariente, and P. R. Griffiths, *Proceedings of the 7th International Conference on Fourier Transform Spectroscopy,* SPIE Volume 1145 (SPIE, Bellingham, Washington, 1989), p. 476.
14. C. J. Manning, R. A. Palmer, J. L. Chao, C. Marcott, and I. Noda, Appl. Spectrosc. **45,** 12 (1991).
15. C. J. Manning, R. A. Palmer, and J. L. Chao, Rev. Sci. Instrum. **62,** 1219 (1991).
16. J. H. Perkins and P. R. Griffith, *Proceedings of the 7th International Conference on Fourier Transform Spectroscopy,* SPIE Volume 1145 (SPIE, Bellingham, Washington, 1989), p. 360.
17. M. A. Afromowitz, P. S. Yeh, and S. Yee, J. Appl. Phys. **48,** 209 (1977).
18. Y. Fujii, A. Moritani, and J. Nakai, Jpn. J. Appl. Phys. **20,** 361 (1981).
19. M. Morita, Jpn. J. Appl. Phys. **20,** 835 (1981).
20. M. J. Adams, B. C. Breadle, A. A. King, and G. F. Kirkbright, Analyst **101,** 553 (1976).
21. M. J. Adams and G. F. Kirkbright, Analyst **102,** 281 (1977).
22. B. Mongeau, G. Rousset, and L. Bertrand, Can. J. Phys. **64,** 1056 (1986).
23. A. Rosencwaig, *Photoacoustics and Photoacoustic Spectroscopy* (John Wiley and Sons, New York, 1980).
24. A Mandelis, Y. C. Teng, and B. S. H. Royce, J. Appl. Phys. **50,** 7138 (1979).
25. *Handbook of Common Polymers,* W. J. Roff and J. R. Scott, Eds. (Butterworth & Co., London, 1971).
26. C. L. Choy and K. Young, Polymer **18,** 769 (1977).
27. *Polymer Handbook,* J. Bandrup and E. H. Inmergut, Eds. (Wiley, New York, 1989), 3rd ed.
28. DuPont trade literature.
29. D. Betteridge and P. J. Meyler, Fresenius Z. Anal. Chem. **300,** 337 (1980).
30. D. Betteridge, T. Lilley, and P. J. Meyler, Fresenius Z. Anal. Chem. **296,** 28 (1979).